

Antiferromagnetism induced by non-magnetic dopants in coupled spin–Peierls chains

This article has been downloaded from IOPscience. Please scroll down to see the full text article.

2004 J. Phys.: Condens. Matter 16 6747

(<http://iopscience.iop.org/0953-8984/16/37/010>)

View [the table of contents for this issue](#), or go to the [journal homepage](#) for more

Download details:

IP Address: 129.252.86.83

The article was downloaded on 27/05/2010 at 17:33

Please note that [terms and conditions apply](#).

Antiferromagnetism induced by non-magnetic dopants in coupled spin–Peierls chains

Nicolas Laflorencie¹, Didier Poilblanc¹ and Anders W Sandvik²

¹ Laboratoire de Physique Théorique, CNRS-UMR5152, Université Paul Sabatier, F-31062 Toulouse, France

² Department of Physics, Åbo Akademi University, Porthansgatan 3, FIN-20500 Turku, Finland

Received 26 April 2004

Published 3 September 2004

Online at stacks.iop.org/JPhysCM/16/6747

doi:10.1088/0953-8984/16/37/010

Abstract

Starting from a microscopic model of coupled frustrated spin-1/2 chains, we study the effect of doping with static non-magnetic impurities. The effective interaction between the $S = \frac{1}{2}$ moments induced by the dopants is analysed. This interaction is non-frustrated and extended in space. The picture is applied to the antiferromagnetic long-range ordering observed in spin–Peierls compounds such as CuGeO_3 doped with non-magnetic impurities. The effective diluted long-range Heisenberg spin- $\frac{1}{2}$ model is studied using the stochastic series expansion (SSE) quantum Monte Carlo algorithm. Simulations at extremely low temperature on square lattices with up to 96×96 sites are carried out to investigate the AF ordering down to impurity concentrations x as low as $x \approx 0.02$.

1. Introduction

Doping a spin–Peierls (SP) system with non-magnetic impurities leads to fascinating low-temperature properties. For instance, in the doped quasi-one-dimensional compound $\text{Cu}_{1-x}\text{M}_x\text{GeO}_3$ ($M = \text{Zn}$ or Mg), the discovery of coexistence between dimerization and antiferromagnetic (AF) long-range order (LRO) at small impurity concentration x has motivated extensive experimental [1] and theoretical [2] investigations. Impurity-induced AF LRO has also been observed in other doped spin-gapped materials such as the two-leg ladder $\text{Sr}(\text{Cu}_{1-x}\text{Zn}_x)_2\text{O}_3$ [3], the Haldane compound $\text{Pb}(\text{Ni}_{1-x}\text{Mg}_x)_2\text{V}_2\text{O}_8$ [4], and the coupled spin-dimer system $\text{TlCu}_{1-x}\text{Mg}_x\text{Cl}_3$ [5]. In doped SP materials, frustration and inter-chain couplings are necessary to understand the impurity-induced AF ordering. Within a realistic model including an elastic coupling to a 2D lattice [6], it was shown that a non-magnetic dopant leads to a local magnetic moment in its vicinity. Such moments experience a non-frustrated interaction that could lead, at $T = 0$, to a finite staggered magnetization [7]. Recently, similar conclusions were reached using a model with purely magnetic interactions including a four-spin cyclic exchange coupling [8].

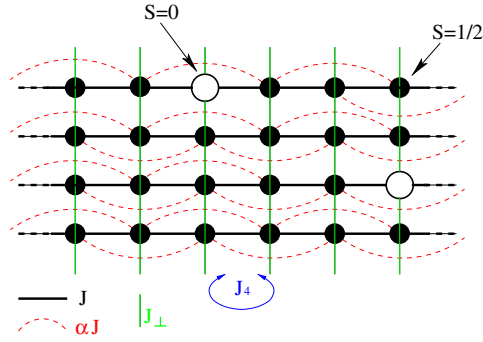


Figure 1. Schematic picture of the coupled chain model with nearest-neighbour (NN), next-nearest-neighbour (NNN), inter-chain, and four-spin couplings J , αJ , J_{\perp} , and J_4 . Full and open circles represent magnetic spin- $\frac{1}{2}$ and non-magnetic dopant sites, respectively.

(This figure is in colour only in the electronic version)

In the following we report numerical studies of a generic model for doped coupled frustrated spin chains [8, 9]. After a presentation of the microscopic description of the coupled SP chains in section 2, we focus in section 3 on the formation of local moments induced by doping and report exact diagonalization (ED) results for the effective magnetic coupling between two released spin- $\frac{1}{2}$ moments. In section 4 we use results of section 3 to construct an effective diluted $S = \frac{1}{2}$ model. We take advantage of the non-frustrated character of the resulting Hamiltonian and perform extensive SSE simulations on 2D lattices as large as 96×96 with up to $N_s = 256$ (dopant) spins, down to temperature as low as $T/J = 1/\beta = 2^{-18}$. The $T = 0$ staggered magnetization as well as the Néel temperature (assuming a small 3D coupling treated using the RPA) are shown versus dopant concentration. We conclude with a brief summary in section 5.

2. Generic microscopic description of coupled SP chains

We start with a microscopic Hamiltonian describing a 2D array of coupled frustrated spin- $\frac{1}{2}$ chains (see figure 1),

$$H = \sum_{i,a} [J(1 + \delta_{i,a}) \mathbf{S}_{i,a} \cdot \mathbf{S}_{i+1,a} + \alpha J \mathbf{S}_{i,a} \cdot \mathbf{S}_{i+2,a} + h_{i,a} S_{i,a}^z], \quad (1)$$

where the i and a indices label the L sites and M chains respectively. The energy scale is set by the exchange coupling along the chains ($J = 1$), and α is the relative magnitude of the next-nearest-neighbour frustrating magnetic coupling. Randomly located dopants (see figure 1) are simply described as inert sites (i, a) where $\mathbf{S}_{i,a} = \mathbf{0}$ is set in equation (1). Small inter-chain couplings are included here in a mean-field self-consistent treatment,

$$h_{i,a} = J_{\perp} (\langle S_{i,a+1}^z \rangle + \langle S_{i,a-1}^z \rangle), \quad (2)$$

$$\delta_{i,a} = \frac{J_4}{J} \{ \langle \mathbf{S}_{i,a+1} \cdot \mathbf{S}_{i+1,a+1} \rangle + \langle \mathbf{S}_{i,a-1} \cdot \mathbf{S}_{i+1,a-1} \rangle \}. \quad (3)$$

While the first term accounts for first-order effects in the inter-chain magnetic coupling J_{\perp} , the second term might originate from a four-spin cyclic exchange process [8]. At a qualitative level, J_4 can also mimic higher-order effects in J_{\perp} [10] or the coupling to a 2D (or 3D) lattice [6].

In the pure case (i.e., without impurities), all the chains are equivalent and the problem is therefore reduced to a single-chain problem in a staggered magnetic field $h_i = -2J_{\perp} \langle S_i^z \rangle$

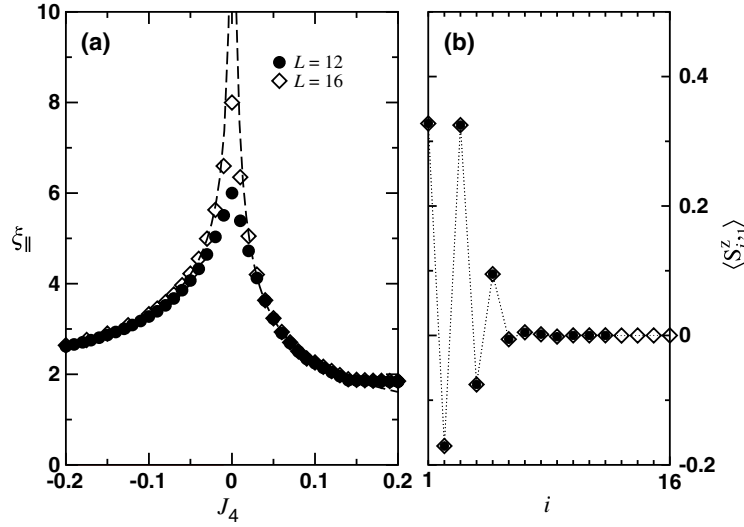


Figure 2. (a) ED data of the soliton average position versus J_4 calculated for $\alpha = 0.5$ and $J_\perp = 0.1$. Different symbols are used for $L \times M = 12 \times 6$ and 16×8 clusters. The long-dashed curve is a power-law fit. (b) Magnetization profile in the doped ($a = 1$) chain at $J_4 = 0.08$, i.e. $\xi_{\parallel} \simeq 2.5$ (adapted from [8]).

and with its NN exchange modulated $\delta J_i = J_4 \langle \vec{S}_i \cdot \vec{S}_{i+1} \rangle$ if $J_4 < 0$ or $\delta J_i = J_4 \langle \vec{S}_{i+1} \cdot \vec{S}_{i+2} \rangle$ if $J_4 > 0$. Using Lanczos ED to solve the MF procedure [11], we identify two different phases in the (α, J_\perp) plane: a dimerized SP phase and an AF ordered phase separated by a transition line $J_\perp = J_\perp^c(\alpha)$ (see figure 2 of [8]). Both the frustration α (for $\alpha > \alpha_c \simeq 0.24$ [12]) and J_4 stabilize the SP phase. Note that $J_\perp^c(\alpha) \rightarrow 0$ when $\alpha \rightarrow \alpha_c$ at the quantum critical point (QCP). In the following all the calculations will be performed at $\alpha = 0.5$ and $J_\perp = 0.1$ which corresponds to a dimerized SP ground state (GS) in the parameter space (α, J_\perp) .

3. Formation of local moments by doping

In the doped case, following the method used in [7], the MF equations are solved self-consistently on finite $L \times M$ clusters and lead to a non-uniform solution. At each step of the MF iteration procedure, we use Lanczos ED techniques to treat *exactly* (although independently) the M *non-equivalent* finite chains and compute $\langle S_{i,a}^z \rangle$ and $\langle \mathbf{S}_{i,a} \cdot \mathbf{S}_{i+1,a} \rangle$ for the next iteration step until convergence is eventually achieved [11]. As found in [8], the soliton confinement is controlled by the J_4 coupling. The confinement length in the chain direction, defined as $\xi_{\parallel} = \sum_i i |S_i^z| / \sum_i |S_i^z|$, ‘measures’ the average position of the magnetic moment from the dopant site and follows a power law $\xi_{\parallel} \sim J_4^{-\eta}$ (see figure 2). Qualitatively, it means that by breaking a dimer each impurity releases an effective localized spin $\frac{1}{2}$ (see figure 3). At very low temperature (i.e. below the temperature scale set by the spin gap of the undoped system) the physics is then dominated by these effective spin- $\frac{1}{2}$ degrees of freedom.

The effective magnetic coupling between two impurities (located at random positions in the system) is given by the singlet–triplet gap $J^{\text{eff}}(\Delta i, \Delta a) = E(S = 1) - E(S = 0)$, Δi (Δa) being the relative dopant separation in the longitudinal (transverse) direction. One of our key results is the non-frustrated character of this effective coupling (although the original model is frustrated) and its long-distance behaviour. In figure 4, the magnitude $|J^{\text{eff}}|$ is plotted

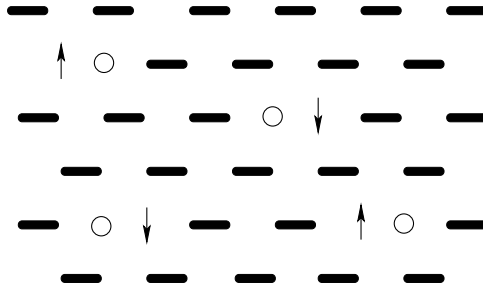


Figure 3. Schematic picture of a doped SP system. Thick bonds correspond to dimers, and the non-magnetic dopants are represented by open circles. The spin- $\frac{1}{2}$ moments released by the dopants are shown as arrows.

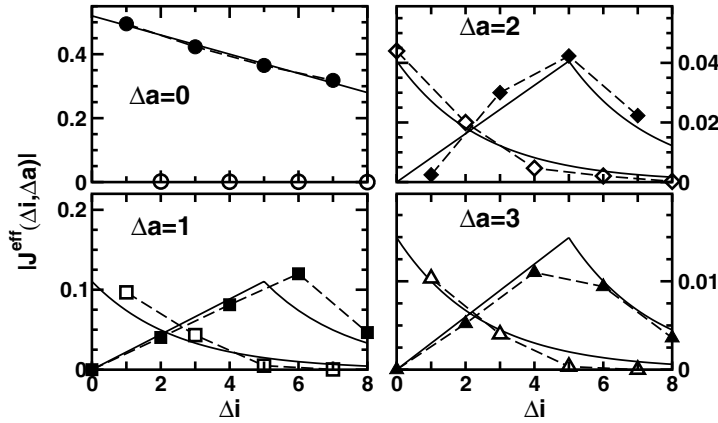


Figure 4. Magnitude of J^{eff} versus separation (Δi , Δa) computed by ED on an $L \times M = 16 \times 8$ system with $\alpha = 0.5$, $J_{\perp} = 0.1$ and $J_4 = 0.08$. Closed (open) symbols correspond to AF (F) interactions. The solid curves are fits, discussed in [9].

versus the impurity separation in the chain direction Δi for different separations $\Delta a = 0-3$ in the transverse direction. Using only five phenomenological parameters, two energy scales and three length scales, we have been able to fit the ED data for a wide range of physical parameters (see [9]).

4. Quantum Monte Carlo study of AF ordering

The computed non-frustrating long-ranged magnetic two-body interaction is used to construct an effective Heisenberg model of randomly located spin- $\frac{1}{2}$ objects on a $\mathcal{N} = L \times L$ square lattice

$$\mathcal{H}^{\text{eff}} = \sum_{\mathbf{r}_1, \mathbf{r}_2} \epsilon_{\mathbf{r}_1} \epsilon_{\mathbf{r}_2} J^{\text{eff}}(\mathbf{r}_1 - \mathbf{r}_2) \mathbf{S}_{\mathbf{r}_1} \cdot \mathbf{S}_{\mathbf{r}_2}, \quad (4)$$

with $\epsilon_{\mathbf{r}} = 1$ (0) with probability x ($1-x$), where x is the dopant concentration. Note that one implicitly assumes that three- or multiple-spin interactions can be neglected. This model has been studied with the SSE method [13]. In this approach, the interactions are sampled stochastically, and for a long-ranged interaction the computational effort is then reduced from $\sim N_s^2$ ($N_s = x\mathcal{N}$ being the number of spins) to $N_s \ln(N_s)$ [14]. In order to accelerate the

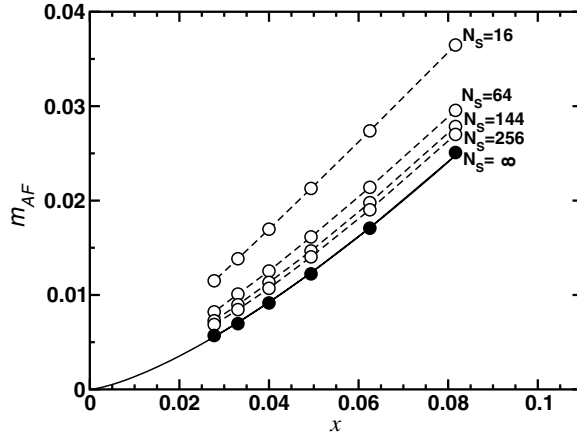


Figure 5. Doping dependence of m_{AF} for various numbers of spins (as shown on the plot) and in the thermodynamic limit (full symbols). The solid curve corresponds to a power law fit giving $m_{\text{AF}} \simeq 0.796x^{1.38}$.

convergence of the simulations at the very low temperatures needed to approach the GS, we use a β -doubling scheme [15] where the inverse temperature is successively increased by a factor of two. An almost equilibrated starting configuration for a new β can then be obtained by ‘doubling’ the last configuration generated at the previous β . Comparing results at several $\beta = 2^n$, one can subsequently check that the $T \rightarrow 0$ limit has been reached.

The AF ordering instability is signalled by the divergence with system size of the staggered structure factor,

$$S(\pi, \pi) = \frac{1}{\mathcal{N}} \left\langle \left(\sum_i (-1)^i S_i^z \right)^2 \right\rangle, \quad (5)$$

where i labels the sites, magnetic or non-magnetic, on the 2D lattice. In the present diluted model, it is more convenient to define a staggered structure factor per site $s(\pi, \pi) = S(\pi, \pi)/\mathcal{N}$ which should converge in an ordered AF state. The (finite-size) sublattice magnetization m_{AF} can then be obtained by averaging $s(\pi, \pi)$ over a large number of dopant distributions, i.e., $(m_{\text{AF}})^2 = 3 \langle s(\pi, \pi) \rangle_{\text{dis}}$, where the factor of three comes from the spin-rotational invariance [16] and $\langle \dots \rangle_{\text{dis}}$ stands for the disorder average, which we have performed using at least 2000 random samples.

Since, strictly speaking, ordering in 2D occurs at $T = 0$ ($\beta = \infty$) we have first converged each simulation to $T = 0$ using the β -doubling scheme [15]. Then, using a polynomial fit in $1/\sqrt{N_s}$ (order two is sufficient) an accurate extrapolation to the thermodynamic limit, $N_s \rightarrow \infty$ (or $L \rightarrow \infty$ at constant x), has been performed. The doping dependence of the extrapolated m_{AF} is given in figure 5. We have tested various fits of the data. A power law $\propto x^\mu$ gives an exponent $\mu \simeq 1.4 > 1$, which implies a magnetization per dopant $m_{\text{spin}} \sim x^{0.4}$ which vanishes in the $x \rightarrow 0$ limit. However, alternative forms, e.g., $a_1x + a_2x^2$, cannot be ruled out.

We finish this investigation by calculating the Néel temperature, assuming a small (effective) 3D magnetic coupling $\lambda_{3\text{D}}$ between the planes. Using an RPA criterion, the critical temperature T_N is simply given by $\chi_{\text{stag}}(T_N) = 1/|\lambda_{3\text{D}}|$ where the staggered spin susceptibility (normalized per site) is defined as usual by

$$\chi_{\text{stag}}(T) = \frac{1}{\mathcal{N}} \sum_{i,j} (-1)^{r_i+r_j} \int_0^\beta d\tau \langle S_i^z(0) S_j^z(\tau) \rangle, \quad (6)$$

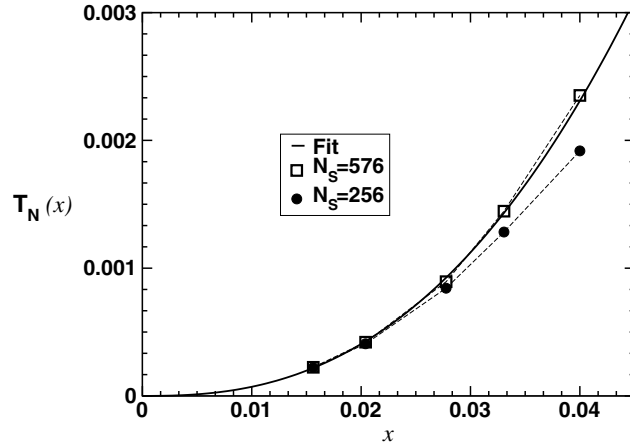


Figure 6. Néel temperature versus dopant concentration x for a 3D RPA inter-plane coupling $\lambda_{3D} = 0.02$ and for $N_s = 256$ and 576 spins. The solid curve is a fit to the form $T_N \simeq 7.37 \times x^{2.507}$ for $N_s = 576$.

and is averaged over several disorder configurations (typically 2000). Since $\chi_{\text{stag}}(T_N)$ is expected to reach its thermodynamic limit for a *finite* linear size L as long as T_N remains *finite*, accurate values of T_N can be obtained using a finite-size computation of $\chi_{\text{stag}}(T)$ for not too small inter-chain couplings. T_N is determined by the intersection of the curve $\chi_{\text{stag}}(T)$ with a horizontal line at $1/\lambda_{3D}$. The doping dependence of T_N is plotted in figure 6 for a particularly small value $\lambda_{3D} = 0.02$ (for $\lambda_{3D} = 0.01$, see [9]). It clearly reveals a rapid decrease of T_N when $x \rightarrow 0$, but, in agreement with experiments [1], does not suggest a non-zero critical concentration. More precisely, it was shown by Manabe *et al* [17] that the Néel temperature measured in $\text{Cu}_{1-x}\text{Zn}_x\text{GeO}_3$ could be fitted by an exponential law of the form $T_N(x) = A \exp(-B/x)$, with A and B two phenomenological parameters. From our numerical results, one decade is not enough to distinguish an exponential form from a power law.

5. Conclusion

In summary, we have proposed a quite versatile procedure for studying impurities in gapped spin system and illustrated it in the case of doped SP chains. For this system, we have shown that the local moment induced by a dopant is controlled by a J_4 term which might have several origins (magnetic or elastic). Using ED technique to compute the effective interaction between two dopants, an effective low-energy Hamiltonian has been constructed and studied with the SSE method (which is applicable here because of the remarkable non-frustrated nature of the effective model) in combination with finite-size scaling to compute the GS staggered magnetization. Calculations of the staggered susceptibility at finite temperature were used in combination with an RPA treatment of the 3D couplings to study the doping dependence of the Néel temperature. Finally, we emphasize that the procedure developed here could be extended easily to other spin-gapped systems like interacting dimer systems [5], weakly coupled ladders [3] or 2D disordered systems.

References

- [1] Hase M *et al* 1993 *Phys. Rev. Lett.* **71** 4059
- Oseroff S B *et al* 1995 *Phys. Rev. Lett.* **74** 1450
- Regnault L-P *et al* 1995 *Europhys. Lett.* **32** 579

- Masuda T *et al* 1998 *Phys. Rev. Lett.* **80** 4566
Grenier B *et al* 1998 *Phys. Rev. B* **58** 8202
For a topical review see also Uchinokura K 2002 *J. Phys.: Condens. Matter* **14** R195
- [2] Martins G B, Dagotto E and Riera J 1996 *Phys. Rev. B* **54** 16032
Sørensen E S, Affleck I, Augier D and Poilblanc D 1998 *Phys. Rev. B* **58** R14701
Nakamura T 1999 *Phys. Rev. B* **59** R6589
Normand B and Mila F 2002 *Phys. Rev. B* **65** 104411
- [3] Azuma M *et al* 1997 *Phys. Rev. B* **55** R8658
[4] Uchiyama Y *et al* 1999 *Phys. Rev. Lett.* **83** 632
[5] Oosawa A, Ono T and Tanaka H 2002 *Phys. Rev. B* **66** 020405
[6] Hansen P, Augier D, Riera J and Poilblanc D 1999 *Phys. Rev. B* **59** 13557
[7] Dobry A *et al* 1999 *Phys. Rev. B* **60** 4065
[8] Laflorencie N and Poilblanc D 2003 *Phys. Rev. Lett.* **90** 157202
[9] Laflorencie N, Poilblanc D and Sandvik A W 2004 *Phys. Rev. B* **69** 212412
- [10] Chains with (in-phase relative) dimerizations $\propto \delta$ are stabilized by an energy $\propto J_{\perp}^2/J \times \delta$ (per bond); see Byrnes T M R, Murphy M T and Sushkov O P 1999 *Phys. Rev. B* **60** 4057
- [11] For a discussion of the convergence of the iterative procedure, see Laflorencie N and Poilblanc D 2004 Simulations of pure and doped low-dimensional spin-1/2 gapped systems *Quantum Magnetism (Springer Lecture Notes in Physics vol 645)* (Berlin: Springer)
- [12] Okamoto K and Nomura K 1992 *Phys. Lett. A* **169** 433
Eggert S 1996 *Phys. Rev. B* **R54** 9612
- [13] Sandvik A W and Kurkijärvi J 1991 *Phys. Rev. B* **43** 5950
Sandvik A W 1992 *J. Phys. A: Math. Gen.* **25** 3667
Sandvik A W 1999 *Phys. Rev. B* **59** R14157
- [14] Sandvik A W 2003 *Phys. Rev. E* **68** 056701
[15] Sandvik A W 2002 *Phys. Rev. B* **66** 024418
[16] Reger J D and Young A P 1988 *Phys. Rev. B* **37** 5978
[17] Manabe K, Ishimoto H, Koide N, Sasago Y and Uchinokura K 1998 *Phys. Rev. B* **R58** 575